STScI | SPACE TELESCOPE SCIENCE INSTITUTE

Instrument Science Report COS 2018-07(v1)

The Spectral Resolution of the COS FUV channel at Lifetime Position 4

Andrew Fox[1], Bethan James[1], Julia Roman-Duval[1], Marc Rafelski[1], Paule Sonnentrucker[1,2]

[1] Space Telescope Science Institute, 3700 San Martin Drive, Baltimore, MD 21218
[2] European Space Agency

16 February 2018

ABSTRACT In this ISR we report on the COS FUV spectral resolution at Lifetime Position 4 (LP4). We cover five central wavelength (cenwave) settings: G130M/1222, G130M/1291, G130M/1327, G160M/1577, and G160M/1623. We base our analysis on the profiles of narrow interstellar absorption lines in the COS FUV spectra of the SMC star AzV 75. We show that a high-resolution STIS E140M spectrum of AzV 75 convolved with the COS line spread functions (LSFs) generated by Code V optical models can successfully reproduce the observed COS line profiles at LP4. The spectral resolution at LP4 has degraded by ≈10-15% relative to LP3, as expected from the models. The highest resolution achievable is on the FUVA segment of the G160M cenwaves, where it reaches R=19,700 (FWHM=15.2 km s^{-1}) at 1780 Å. The resolution of the workhorse cenwave G130M/1291 varies from R=12 100 (24.8 km s^{-1}) at 1150 Å to R=16 900 (17.7 km s^{-1}) at 1450 Å.

Contents

1. Introduction

On October 2, 2017, routine operations of the COS FUV channel were moved to the fourth Lifetime Position, LP4. This date was chosen to coincide with the start of Cycle 25. All Cycle 25 COS/FUV observations are now executed by default at LP4, with the exception of the blue modes (G130M/1055 and G130M/1096) that remain at LP2 due to their wide cross-dispersion profiles. The move to LP4 was made in order to mitigate the effect of gain sag and provide the community with access to an unsagged region of the FUV detector. LP4 is located 5.0 arcseconds below LP1 in the cross-dispersion direction, and 2.5 arcseconds below LP3. The move to LP4 was accompanied by a new set of restrictions on detector segment usage, FP-POS settings, and target acquisition settings, that together are known as the COS2025 policies, described at http://www.stsci.edu/hst/cos/cos2025.

Because of off-axis optical effects, the spectral resolution declines as a function of angular separation from LP1, which was located on-axis along the middle of the FUV detector. The magnitude of the decline can be predicted by optical models (as discussed in Section 3), but needs to be verified using LP4 observations of sources with narrow interstellar absorption features in their spectra. The steps taken to conduct this verification, and plots showing the spectral resolution as a function of wavelength for each cenwave, are presented in this ISR.

This report forms one of a pair of ISRs on the COS FUV resolution at LP4 – the companion ISR (Fox 2018) describes the *spatial* resolution of the FUV detector at LP4. Our analysis follow earlier programs to characterize the COS FUV spectral resolution at LP2 (Roman-Duval et al. 2013) and LP3 (Roman-Duval et al. 2017a), and to provide a quick check of the 1291 and 1327 spectral resolution at LP4 (Sonnentrucker et al. 2017b). Another related ISR (James et al. 2018) describes the resolution of the discontinued 1223 cenwave at LP4 (see Roman-Duval et al. 2017b for discussion of why this cenwave was deprecated).

2. Observations

A log of the COS observations analyzed in this ISR is provided in Table 1. The data were taken under two programs: 14842 (PI=P. Sonnentrucker; 1291 and 1327 cenwaves) and 15366 (PI=A. Fox; 1222, 1577, and 1623 cenwaves). The target in both programs was AzV75, a blue supergiant star in the Small Magellanic Cloud with spectral type O5.5I(f). It was chosen for two reasons: (1) it is UV-bright but not too bright for COS, so high signal-to-noise (S/N) ratios can be reached quickly without exceeding the count rate limits for the FUV detector; (2) it is heavily reddened, with $E(B-V)$=0.16, ensuring a high foreground neutral gas column N(H I), which means its spectrum shows many narrow interstellar lines in absorption. Program 14842 was executed in summer 2016

Setting	Prog. ID	Date (UT)	Exposure Time[a] (s)	Dataset ID
G130M/1222	15366	2017-08-10	1552	ldm701010
G130M/1291	14842	2016-08-29	800	ldb301020
G130M/1327	14842	2016-08-29	800	ldb301040
G160M/1577	15366	2017-08-10	2070	ldm701020
G160M/1623	15366	2017-08-10	2070	ldm701030

Table 1. Log of observations for LP4 resolution programs.
[a] Total exposure time combined across FP-POS position.

as part of the LP4 exploratory phase, whereas Program 15366 was executed in summer 2017 in the LP4 calibration phase. The datasets are similar in their S/N properties, with S/N=60 per resolution element when combined over the four FP-POS positions.

3. Code V Optical Models

We examine model predictions for the LP4 spectral resolution generated from the Code V optical code, which uses an optical model of the COS system provided by Tom Delker (Ball Aerospace) and updated by Erin Elliott. The advantage of Code V over ray-trace codes is that it properly characterizes the wings of the COS LSF, which contain a significant fraction of the total power in the profile. The profiles are known to be non-gaussian due to mid-frequency wavefront errors, which are due to polishing errors on the primary and secondary *HST* mirrors (Ghavamian et al. 2009).

All point spread functions (PSFs) for COS are highly astigmatic, i.e. they suffer from off-axis aberrations. For each lifetime position and for each cenwave, the grating positions are chosen so that the PSF on the image plane is as narrow as possible in the dispersion direction, to maximize the spectral resolution. The grating positions are specified by the motor step numbers for the focus motor and the rotation motor. Each focus-motor step (ΔF) leads to a 2.3518μm change in the linear focus position of the grating, while each rotation-motor step (ΔR) leads to a 0.028125° change in the grating tilt (Roman-Duval et al. 2013).

The grating tilt (α) for each cenwave is calculated as the number of rotation steps from nominal ($N_R - N_{R0}$) times the rotation step size (ΔR), plus the nominal tilt location of the grating, α_0:

$$\alpha = (N_R - N_{R0})\Delta R + \alpha_0 \tag{1}$$

The total focus shift ($F_{\rm total}$) for each cenwave can be expressed as a combination of linear and rotational components (Roman-Duval et al. 2013):

$$F_{\rm total} = F_{\rm lin} + F_{\rm rot} = (N_F - N_{F0})\Delta F - 42.8(N_R - N_{R0})\Delta F \tag{2}$$

Grating	Cenwave	Rotation Position N_R (motor steps)	Steps from nominal $N_R - N_{R0}$ (motor steps)	Grating Tilt α (degrees)
G130M	1055	8095	104	−17.1750
G130M	1096	8078	87	−17.6531
G130M	1222	8026	35	−19.1156
G130M	1291	7999	8	−19.8750
G130M	1300	7995	4	−19.9875
G130M	1309	7991	0	−20.1000
G130M	1318	7987	−4	−20.2125
G130M	1327	7983	−8	−20.3250
G160M	1577	11203	8	−19.8750
G160M	1589	11199	4	−19.9875
G160M	1600	11195	0	−20.1000
G160M	1611	11191	−4	−20.2125
G160M	1623	11187	−8	−20.3250
G140L	1105	1598	7	−7.2105
G140L	1230	1591	0	−7.4074
G140L	1280	1590	−1	−7.4355

Table 2. Grating tilt values for COS FUV modes at LP4, as used in Code V models.

Equations (1) and (2) were used to calculate α and $F_{\rm total}$ of each cenwave at LP4. These are tabulated in Tables 2 and 3, and are the basic parameters specifying the Code V models. The models are used to generate line spread functions (LSFs; dispersion direction) and cross-dispersion spread functions (XDSFs) as a function of wavelength for each cenwave. The LSFs and XDSFs are computed as a function of pixel number, and are each normalized such that their integral is equal to one.

Code V models were run using the absolute focus values at each cenwave determined by the LP4 focus sweep programs (Fox et al. 2017, Sonnentrucker et al. 2017a). The models are used to generate line spread functions (LSFs) as a function of wavelength for each cenwave. Figure 1 shows these predicted LSFs for six cenwaves, and for six reference wavelengths within each cenwave (since the LSFs are a function of wavelength). The LSFs are first plotted on a logarithmic scale to emphasize the structure in the wings of the line profiles, and then on a linear scale, to show the structure near line center.

4. Spectral Resolution Determination

To determine the spectral resolution of COS FUV spectra at LP4, we use the procedure described in full in James et al. (2018). It was derived for use in characterizing the G130M/1223 cenwave. The procedure works by analyzing the line profiles of narrow interstellar absorption features in the AzV75 spectrum. The COS data are compared to existing high-resolution STIS E140M data (FWHM=7.0 $\mathrm{km\,s^{-1}}$) of the target. The

Grating	Cenwave	Rot. Foc. Shift $F_{\rm rot}$ (mm)	Foc. Position N_F (motor steps)	Steps from nominal $N_F - N_{F0}$ (motor steps)	Lin. Foc. Shift $F_{\rm lin}$ (mm)	Tot. Foc. Shift $F_{\rm tot}$ (mm)
G130M	1055	10.469	−2200	−2370	5.574	16.042
G130M	1096	8.757	−2100	−2270	5.339	14.096
G130M	1222	3.523	−879	−1049	2.467	5.990
G130M	1291	0.805	52	−118	0.278	1.083
G130M	1300	0.403	222	52	−0.122	0.280
G130M	1309	0.000	392	222	−0.522	−0.522
G130M	1318	−0.403	562	392	−0.922	−1.325
G130M	1327	−0.805	733	563	−1.324	−2.129
G160M	1577	0.805	−108	−64	0.151	0.956
G160M	1589	0.403	62	106	−0.249	0.153
G160M	1600	0.000	232	276	−0.649	−0.649
G160M	1611	−0.403	402	446	−1.049	−1.452
G160M	1623	−0.805	572	616	−1.449	−2.254
G140L	1105	0.705	−413	−383	0.901	1.605
G140L	1230	0.000	−73	−43	0.101	0.101
G140L	1280	−0.101	−24	6	−0.014	−0.115

Table 3. Focus offsets for COS FUV modes at LP4, as used in Code V models.

STIS data have an accurate wavelength zero point and serve as the reference spectrum. A brief summary of the steps followed is:

(1) We downloaded the co-added, calibrated 1-D COS spectra of the target (x1dsum.fits files listed in Table 1) produced by the `calcos` pipeline using the LP4 reference files.
(2) We identified a number of narrow low-ionization interstellar absorption lines in the bandpass of each cenwave, and selected the wavelength regions around these lines (typically a few Angstroms wide). (3) We convolved the STIS E140M reference spectrum with a grid of models of the COS line spread function (LSF) at LP4 generated by the Code V optical code. The central point in the grid contains the nominal LSF at LP4. The other points in the grid contain LSF models that are degraded (to lower resolution) or enhanced (to higher resolution) by up to $\pm$60% compared to the nominal model. (4) We used a χ^2 analysis to minimize the residuals between the models and the observations, and hence to derive the best-fit resolution, for each wavelength region. Specifically, the best-fit resolution is the resolution of the model LSF that when convolved with the STIS data best reproduces the COS LP4 observations.
(5) We plotted the best-fit resolution against wavelength, including the nominal Code V prediction.

Steps (1) to (5) were then repeated for each cenwave. The selected wavelength regions and the χ^2 analysis are shown in Figures 2 (for 1222), 3 (1291), 4 (1327), 5 (1577), and 6 (1623). Figures 7 and 8 show the plots of resolution vs. wavelength derived from the χ^2 analysis.

In Figure 9 we present a summary of the spectral resolution for the validated Code V models at LP4, together with the predictions for the blue modes 1055 and 1096, which remain at LP2. This figure is intended to provide an overview of the resolution obtained with each cenwave. The 1055, 1096, and 1222 cenwaves show resolution curves that peak and then decline on FUVA toward higher wavelengths, whereas the 1291, 1327, 1577, and 1623 settings show resolution curves that increase with wavelength throughout the bandpass. The best resolution available with COS at LP4 is on the FUVA segments of the G160M cenwaves, where it reaches R=19 700 (FWHM=15.2 km s^{-1}) at 1780 Å.

In the appendix we present another set of figures (Figure 10) directly comparing spectra taken at LP3 and LP4, for different wavelength intervals and cenwaves. These figures allow visual inspection of the minor degradation in resolution between the two LPs.

5. Results and Conclusions

The plots of spectral resolution vs. wavelength (Figures 7 and 8), and the summary plot of resolution for different cenwaves (Figure 9) contain the key results from our study. We highlight the main findings here.

1. The 1222 cenwave has good performance on both detector segments, with mean resolutions $\langle R$(FUVB)$\rangle$=11800$\pm$720 and $\langle R$(FUVA)$\rangle$=13600$\pm$1840. The resolution of 1222 peaks on FUVA, longward of Lyman-α, as predicted by the Code V model. This finding was a key part of the COS team's decision to discontinue usage of the 1223 cenwave in October 2017 (Roman-Duval et al. 2017b).

2. The Code V LSFs have been validated for each of five cenwaves analyzed: 1222, 1291, 1327, 1577, and 1623, since our analysis shows that the resolution vs. wavelength curves lie close (within $\approx$10%) to the model predictions in each case. These LSFs therefore offer a good representation of the resolution characteristics of FUV spectra at LP4, and hence are being released to the community[1] (see Figure 9). They can be used for line-profile fitting analyses. The G130M LSFs have been validated with more data than the G160M LSFs due to more available absorption lines below 1400 Å.

3. Overall the resolution at LP4 has declined by 10–15% from LP3, as expected. The best spectral resolution available with COS at LP4 is on the FUVA segments of the G160M cenwaves, where it reaches R=19 700 (FWHM=15.2 km s^{-1}) at 1780 Å.

4. For G130M/1291, the most widely-used of the G130M cenwaves, the resolution rises fairly linearly from R=12 100 (24.8 km s^{-1}) at 1150 Å to R=16 900 (17.7 km s^{-1}) at 1450 Å.

[1]The LP4 LSFs are available online at http://www.stsci.edu/hst/cos/performance/spectral_resolution/.

Change History for COS ISR 2018-07

Version 1: 16 February 2018- Original Document

References

Fox, A., et al. 2017, Instrument Science Report COS 2017-17
Focusing the COS/FUV G160M and G130M Gratings at Lifetime Position 4
Fox, A. 2018, Instrument Science Report COS 2018-08
The Spatial Resolution of the COS FUV channel at Lifetime Position 4
Ghavamian, P., et al. 2009, Instrument Science Report COS 2009-01
Preliminary Characterization of the Post-Launch Line Spread Function of COS
James, B., et al. 2018, Instrument Science Report in prep
Spectral Resolution of the 1223 Central Wavelength Setting
Roman-Duval, J., et al., 2013, Instrument Science Report COS 2013-07,
COS/FUV Spatial and Spectral Resolution at the new Lifetime Position
Roman-Duval, J., et al. 2017a, Instrument Science Report COS 2017-06
Spectral Resolution of the COS/FUV M-gratings at Lifetime Position 3
Roman-Duval, J., et al. 2017b, Technical Information Report COS 2017-01
Reconciling Expectations and Observations of the G130M 1222 and 1223 Resolution
Sonnentrucker, P., et al., 2017a, Instrument Science Report COS 2017-16
FUV Focus Sweep Exploratory Program for COS at LP4
Sonnentrucker, P., et al., 2017b, Instrument Science Report COS 2017-20,
Quick-check of the COS/FUV G130M Spectral Resolution at Lifetime Position 4

Appendix

In this appendix we include a set of figures (Figure 10) that compare small wavelength regions of COS FUV spectra of the target AzV75 taken at LP4 with equivalent data taken at LP3 (from Program ID 13931; Roman-Duval et al. 2017a). One set of six wavelength regions is included for each cenwave. The LP4 model (formed by convolving the STIS E140M data with the LSF; see Section 4) is included for lines longward of 1180 Å (the low-wavelength end of the STIS spectrum). The profiles are all continuum-normalized. These spectra can be visually inspected to show that the degradation in resolution from LP3 to LP4 is slight.

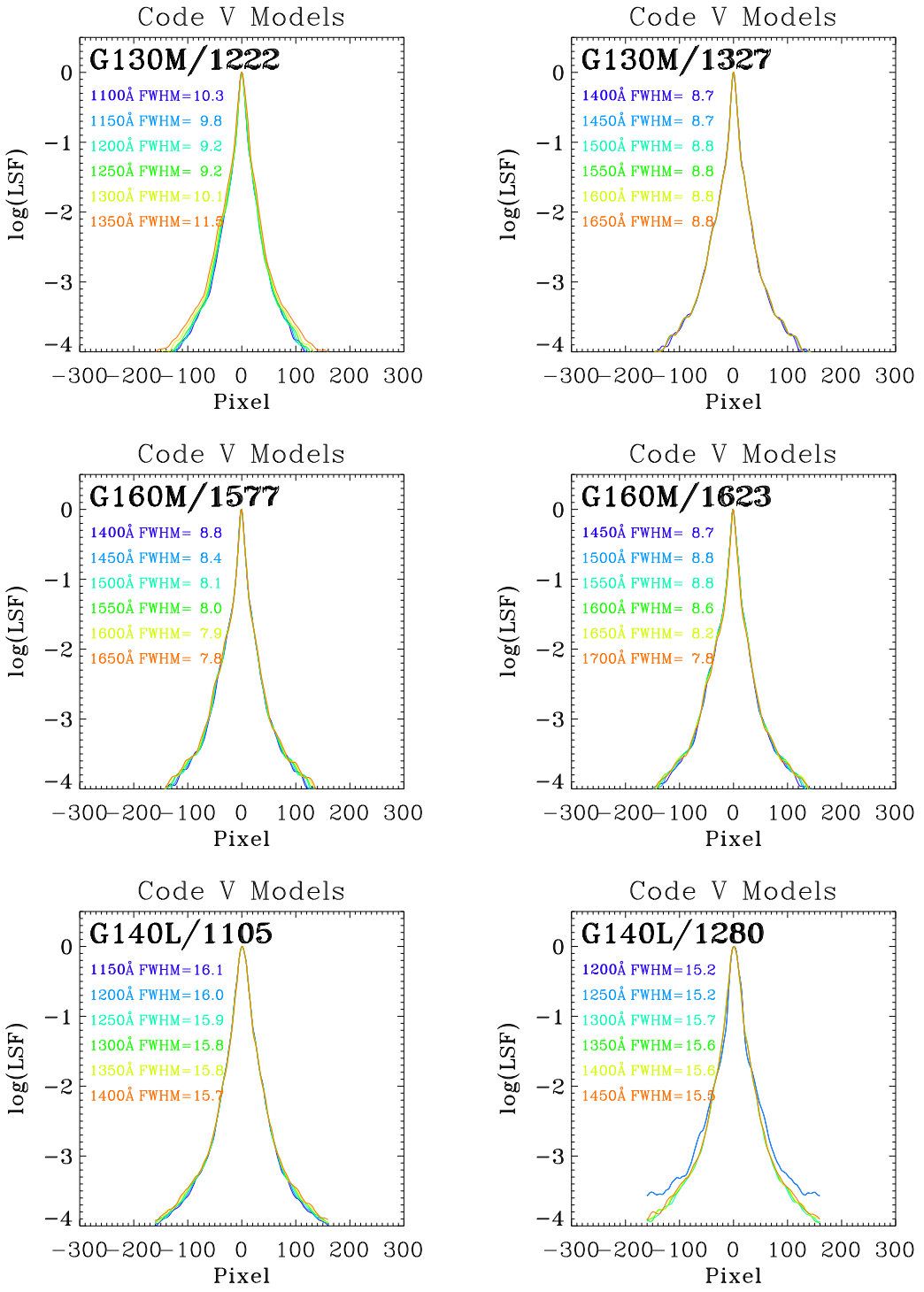

Figure 1. Line spread functions (LSFs) at LP4 predicted by Code V. Two cenwaves are shown for each grating: 1222 and 1327 for G130M, 1577 and 1623 for G160M, and 1105 and 1280 for G140L. Here we show the LSF on a logarithmic scale vs pixel number (see next figure for linear profiles). The FWHM of the profiles at six reference wavelengths is annotated on each panel.

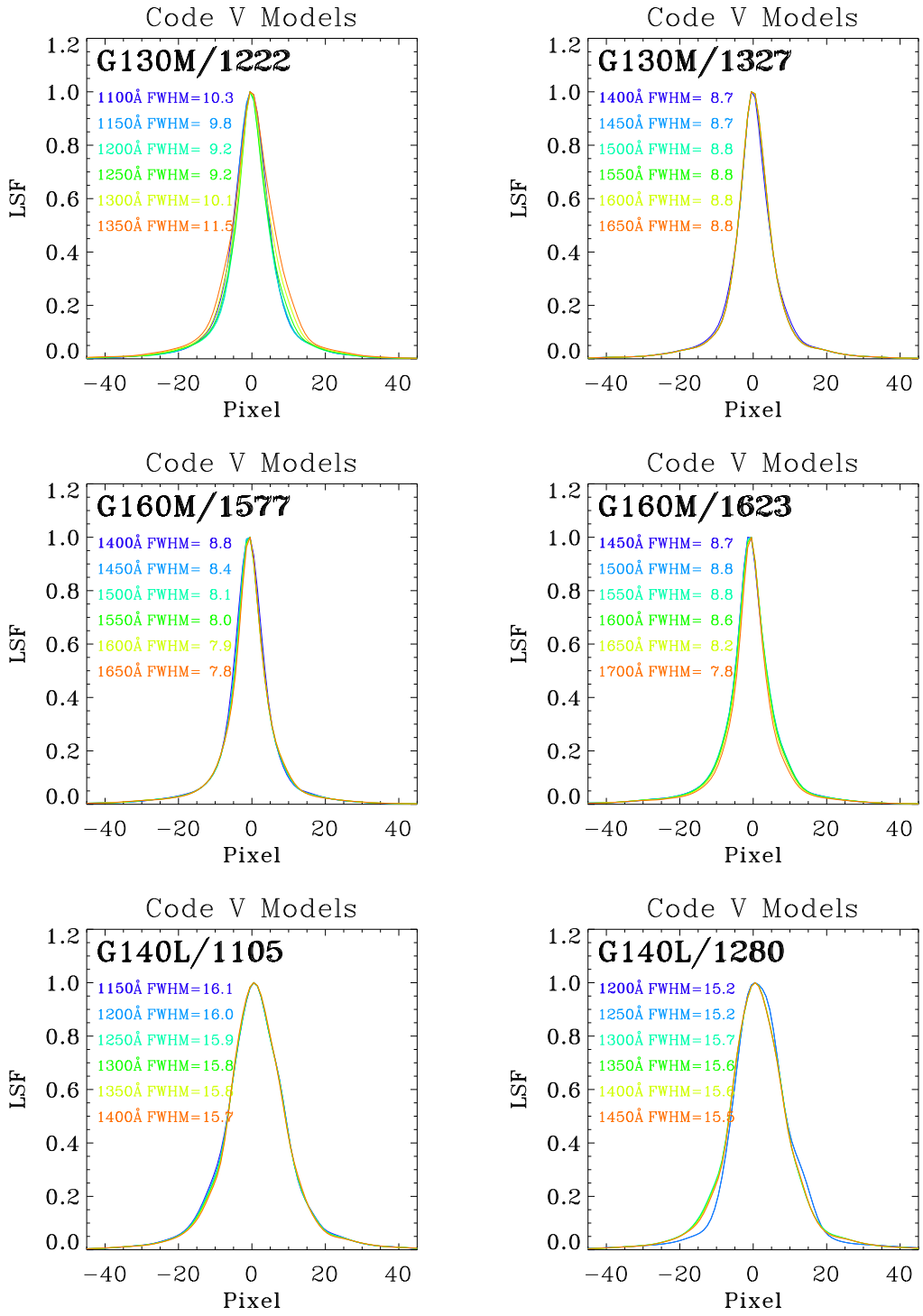

Figure 1. (cont.). Same as the previous figure but with the LSFs on a linear scale. Note the smaller range on the x-axis.

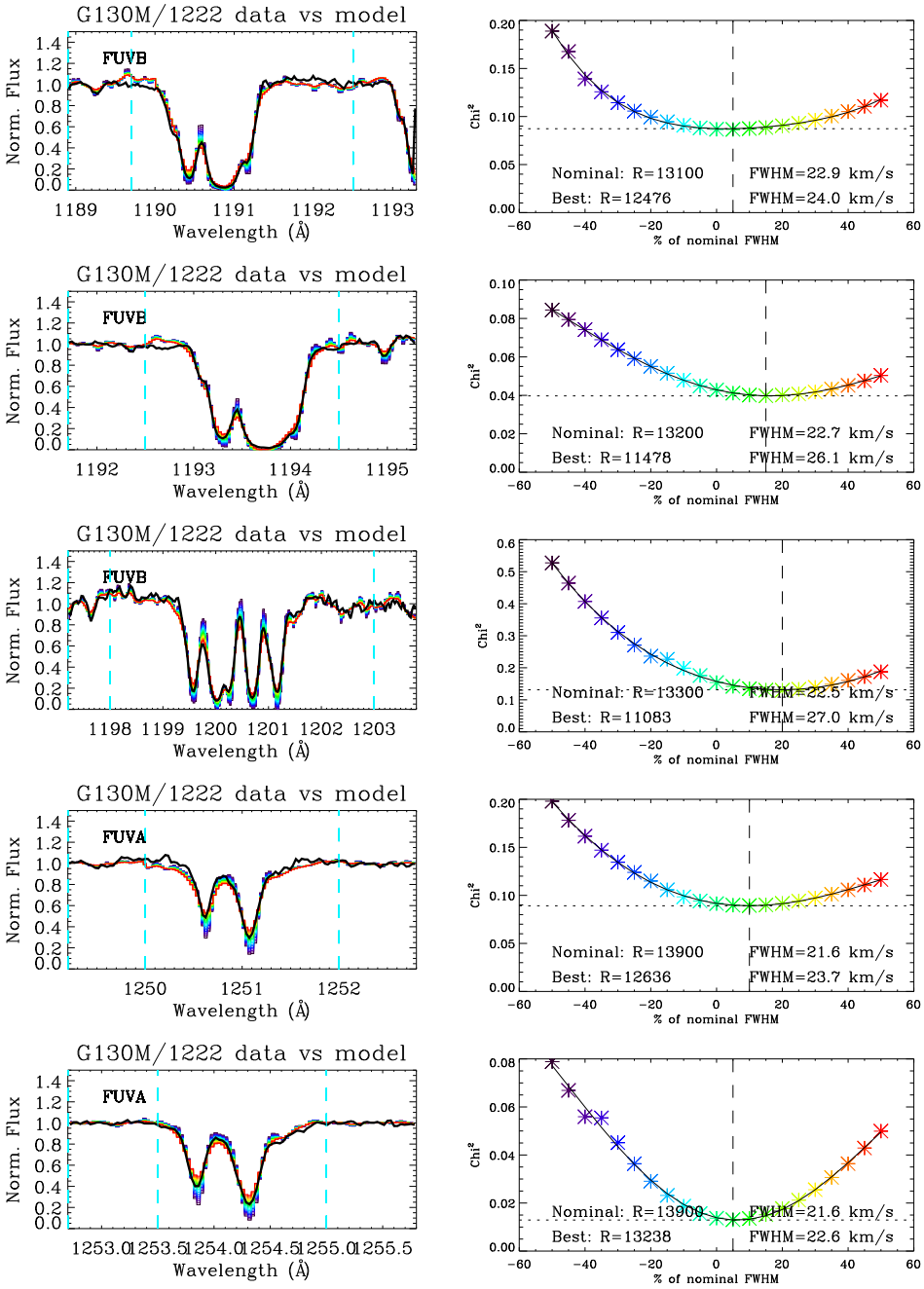

Figure 2. Left: Comparison of G130M/1222 COS data at LP4 (black) with a grid of models at different resolution (solid colored curves) for different wavelength regions. The models are constructed as described in the text. The dashed vertical cyan lines show the continuum normalization regions. **Right:** χ^2 vs. model FWHM as percentage of nominal value. Values of zero on the x-axis correspond to the nominal resolution at that wavelength in the LP4 LSF; negative and positive values correspond to higher and lower spectral resolution, respectively. The nominal and best-fit values of the resolution are annotated on each panel.

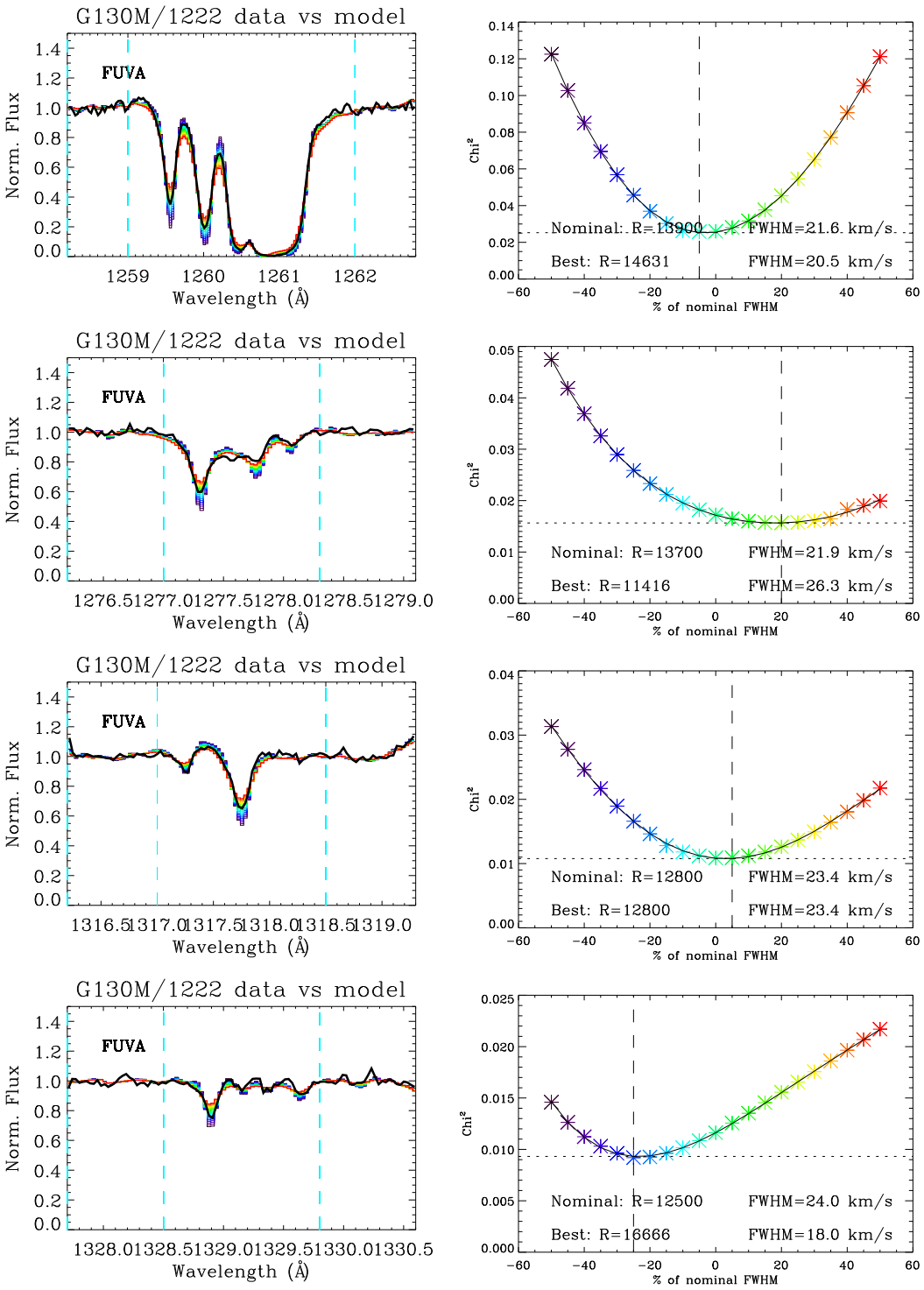

Figure 2. (cont): Remaining four wavelength regions for 1222 resolution analysis.

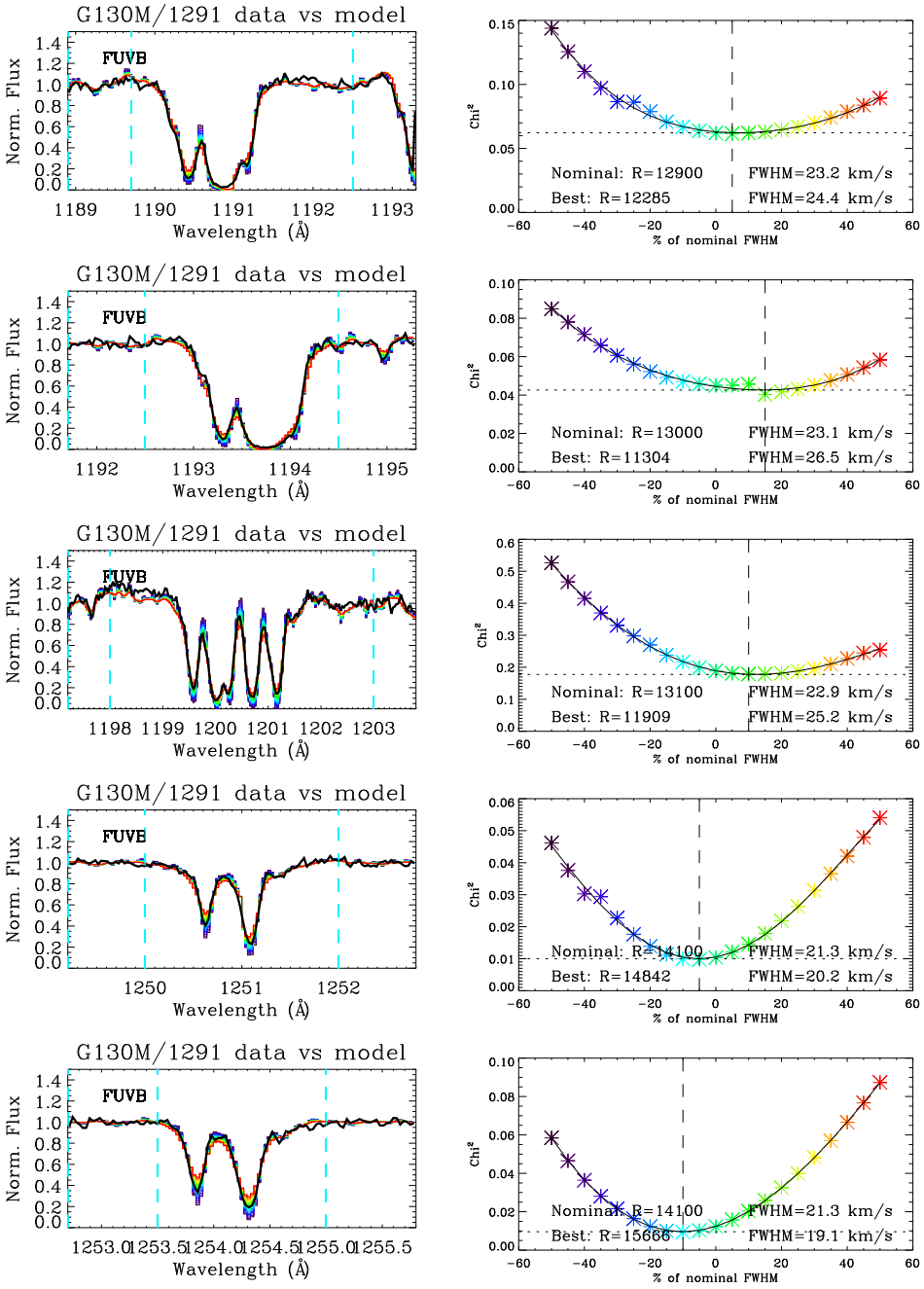

Figure 3. Same as Figure 2, but for the G130M/1291 setting.

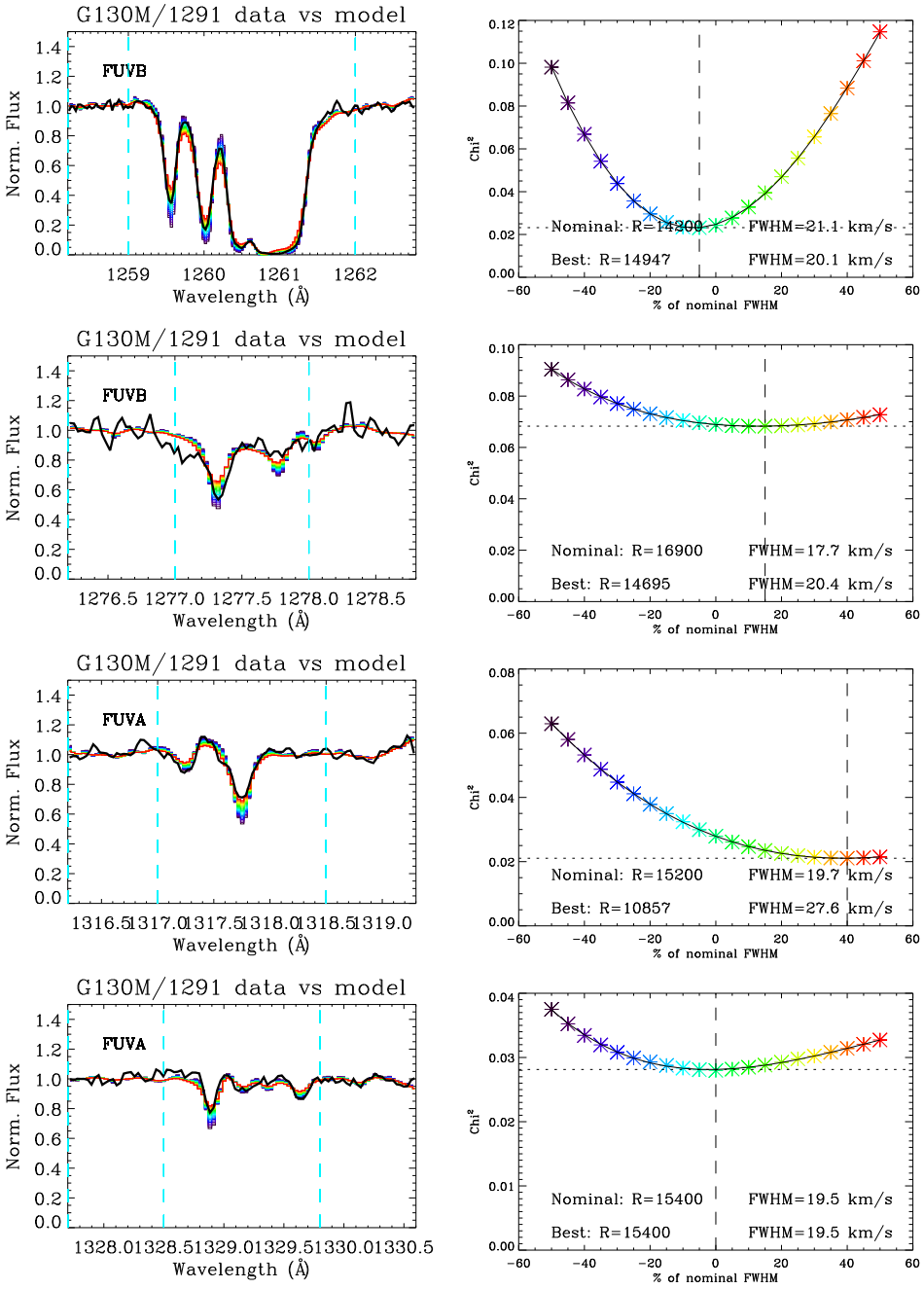

Figure 3. (cont.): Remaining four wavelength regions for 1291 resolution.

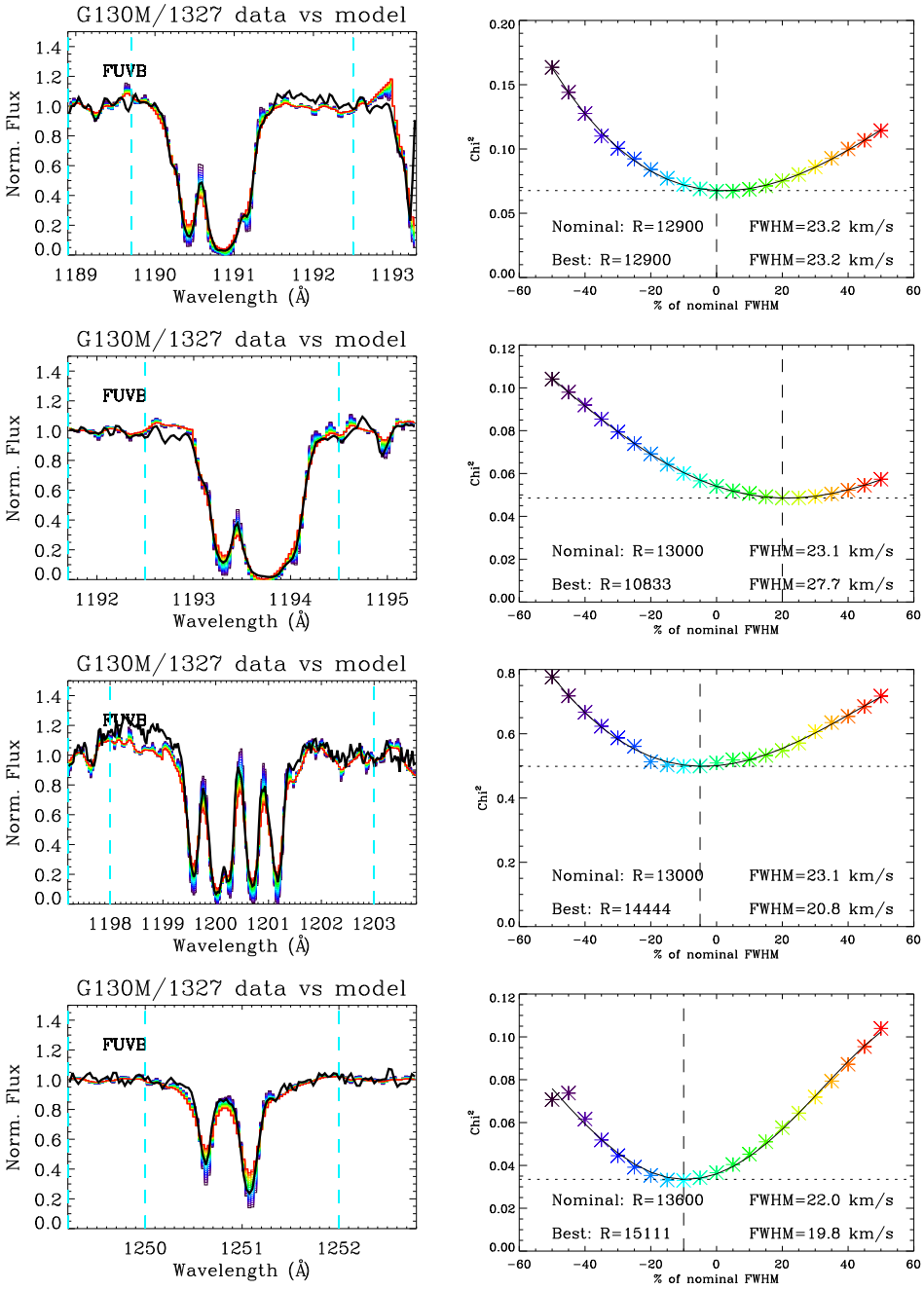

Figure 4. Same as Figure 2, but for the G130M/1327 setting.

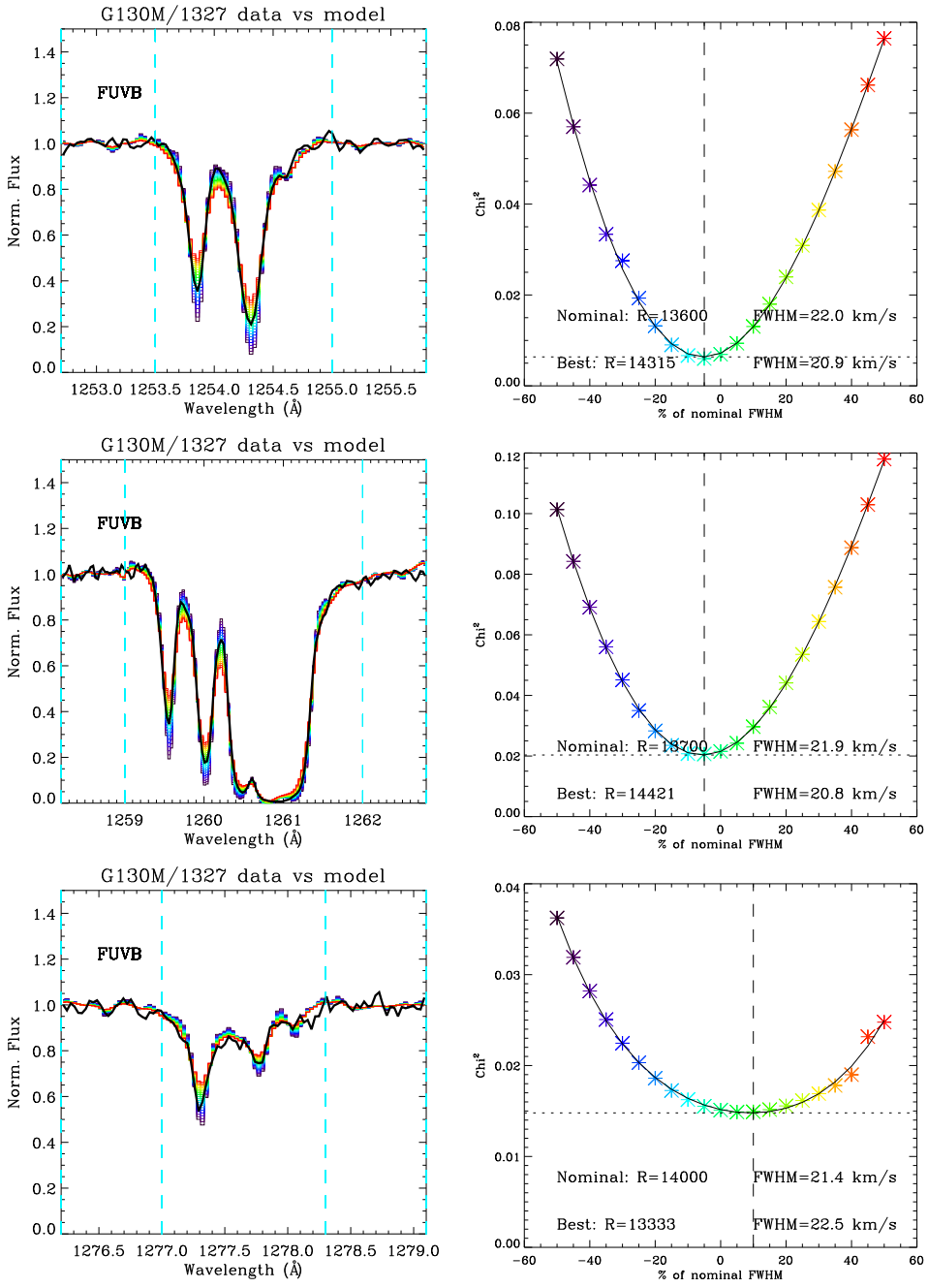

Figure 4. (cont.): Remaining three wavelength regions for 1327 resolution.

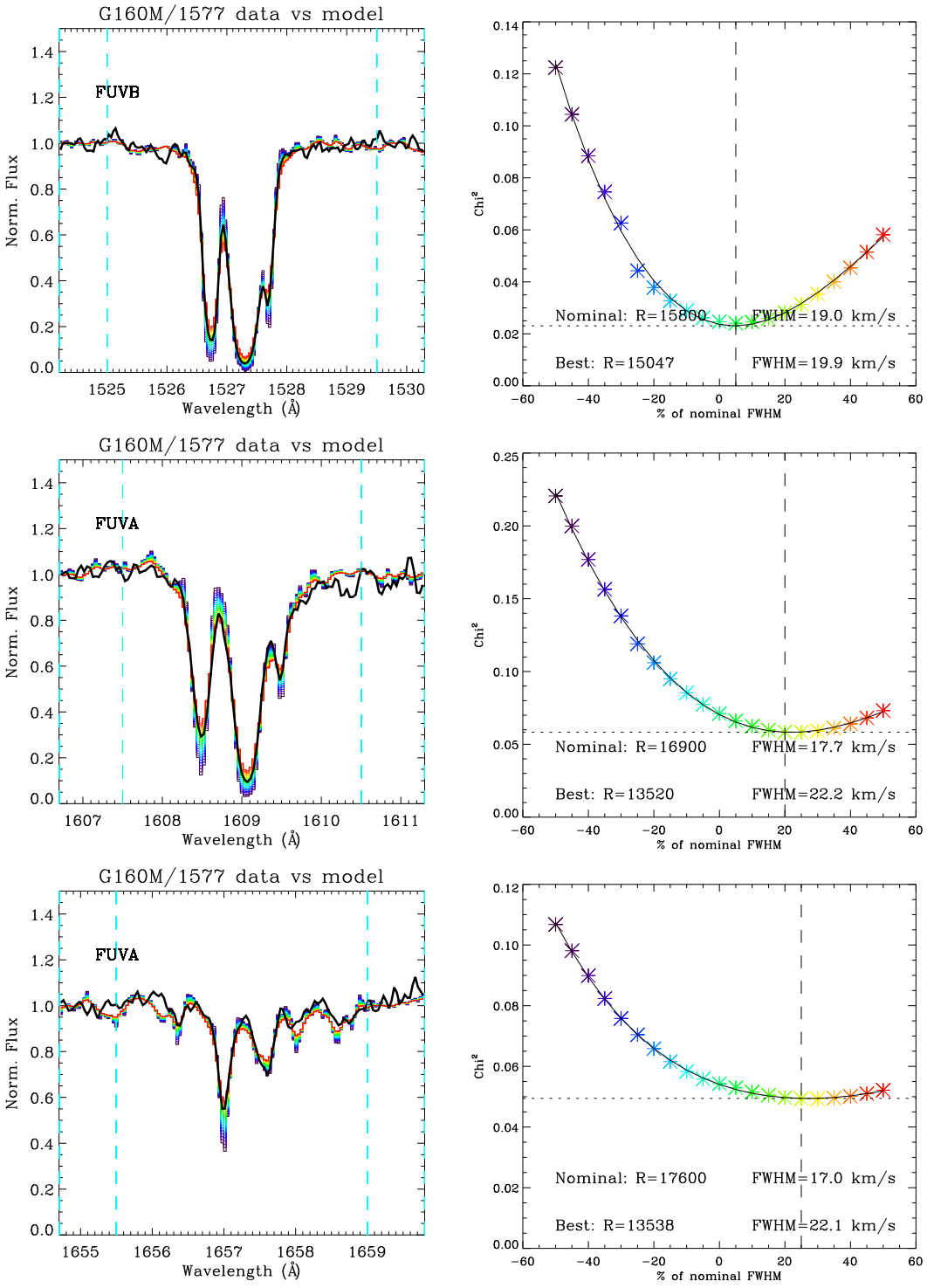

Figure 5. Same as Figure 2, but for the G160M/1577 setting. Only three regions are shown due to a lack of narrow lines in the G160M bandpass.

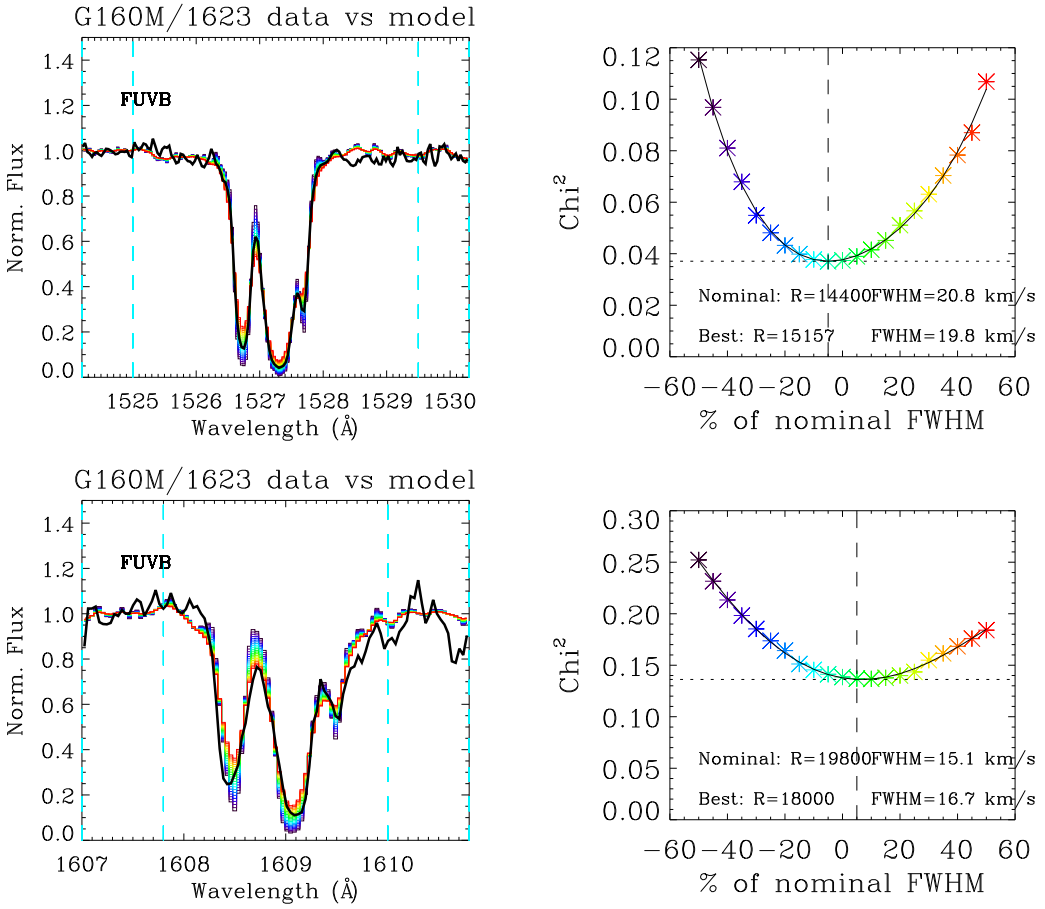

Figure 6. Same as Figure 2, but for the G160M/1623 setting.

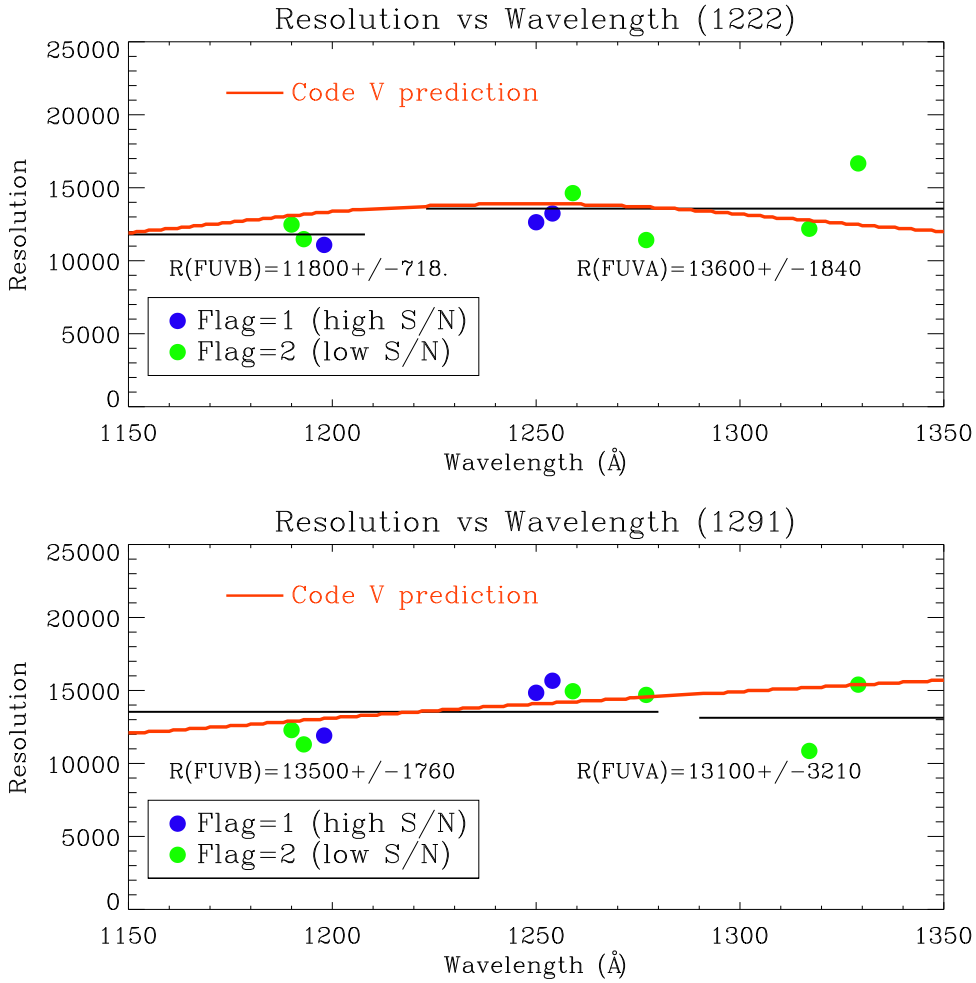

Figure 7. Derived resolution vs. wavelength for G130M/1222 (top) and G130M/1291 (bottom) as obtained by the χ^2-minimization method, for both FUVB (left) and FUVA (right) channels. The mean resolution on each channel is shown with the solid black lines. The data are divided into two groups: Flag=1 (blue) with high S/N, and Flag=2 (green) with low S/N, with the higher S/N lines having higher weight in the final resolution. The prediction from the Code V model is shown as a solid red line.

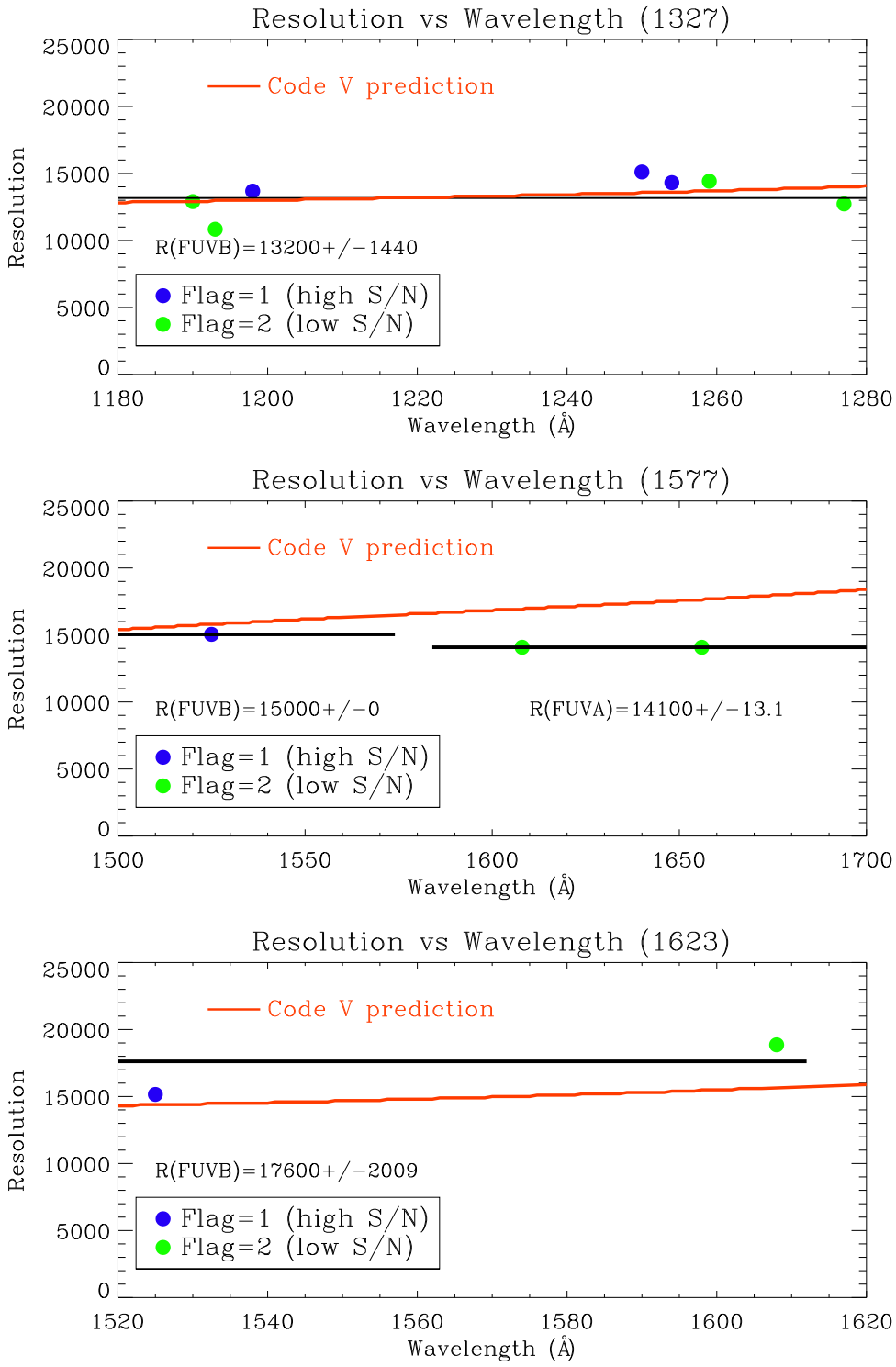

Figure 8. Same as Figure 7, but for G130M/1327 (top), G160M/1577 (middle) and G160M/1623 (bottom). There are fewer data points shown in the lower two panels since there are fewer narrow interstellar absorption lines in the G160M bandpass than in the G130M bandpass.

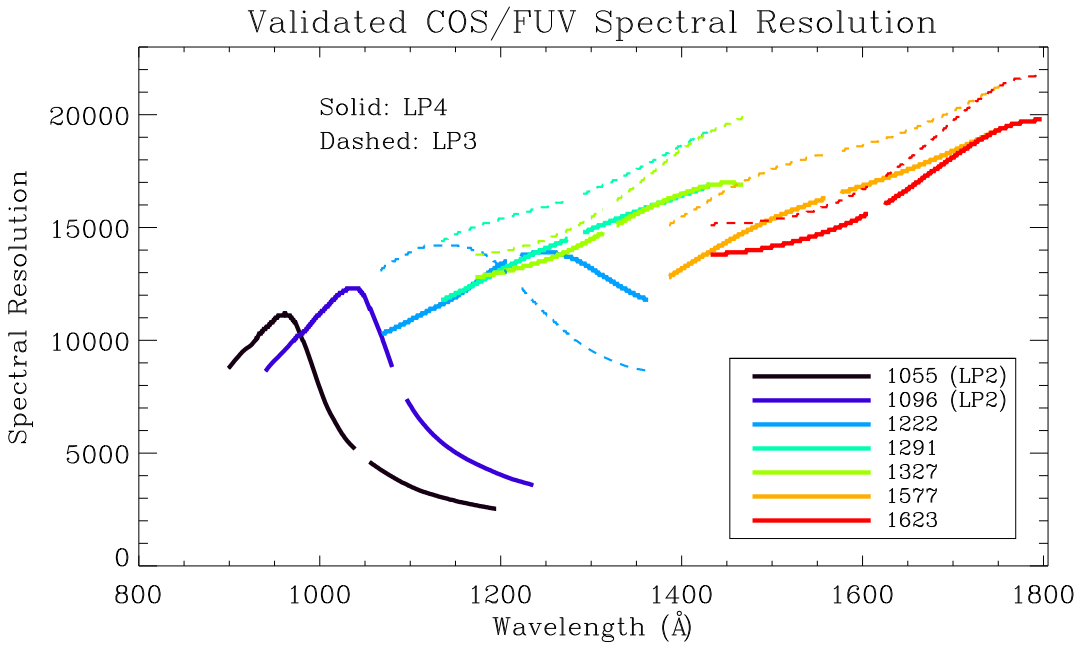

Figure 9. Summary of spectral resolution vs. wavelength at LP4 for the five cenwaves characterized in this ISR (solid lines). The curves show the Code V model predictions that have been validated by comparison with the observations. We include G130M/1055 and G130M/1096 (the "blue modes"), which are taken at LP2. We also include the LP3 model resolution with dashed lines. The gaps in the center of each curve show the gaps between segments FUVB and FUVA.

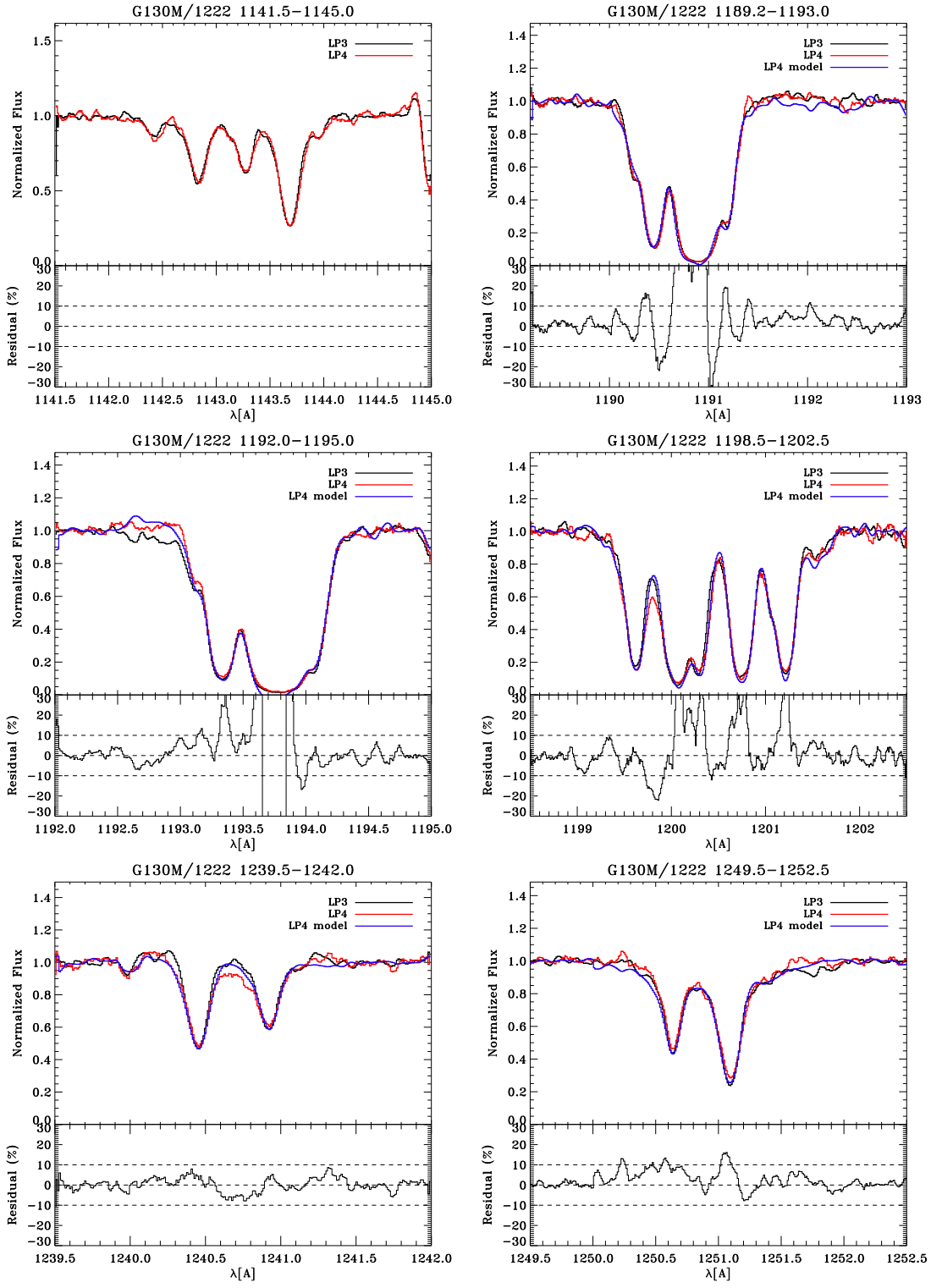

Figure 10. Comparison of COS G130M/1222 spectra of AzV75 taken at LP4 (red) and LP3 (black). Each panel shows a different wavelength interval. The blue line shows the LP4 model (formed by convolving the STIS E140M data with the COS LSF; the model only exists for $\lambda > 1180$ Å). The residual between the LP4 data and the model is shown in the lower panel.

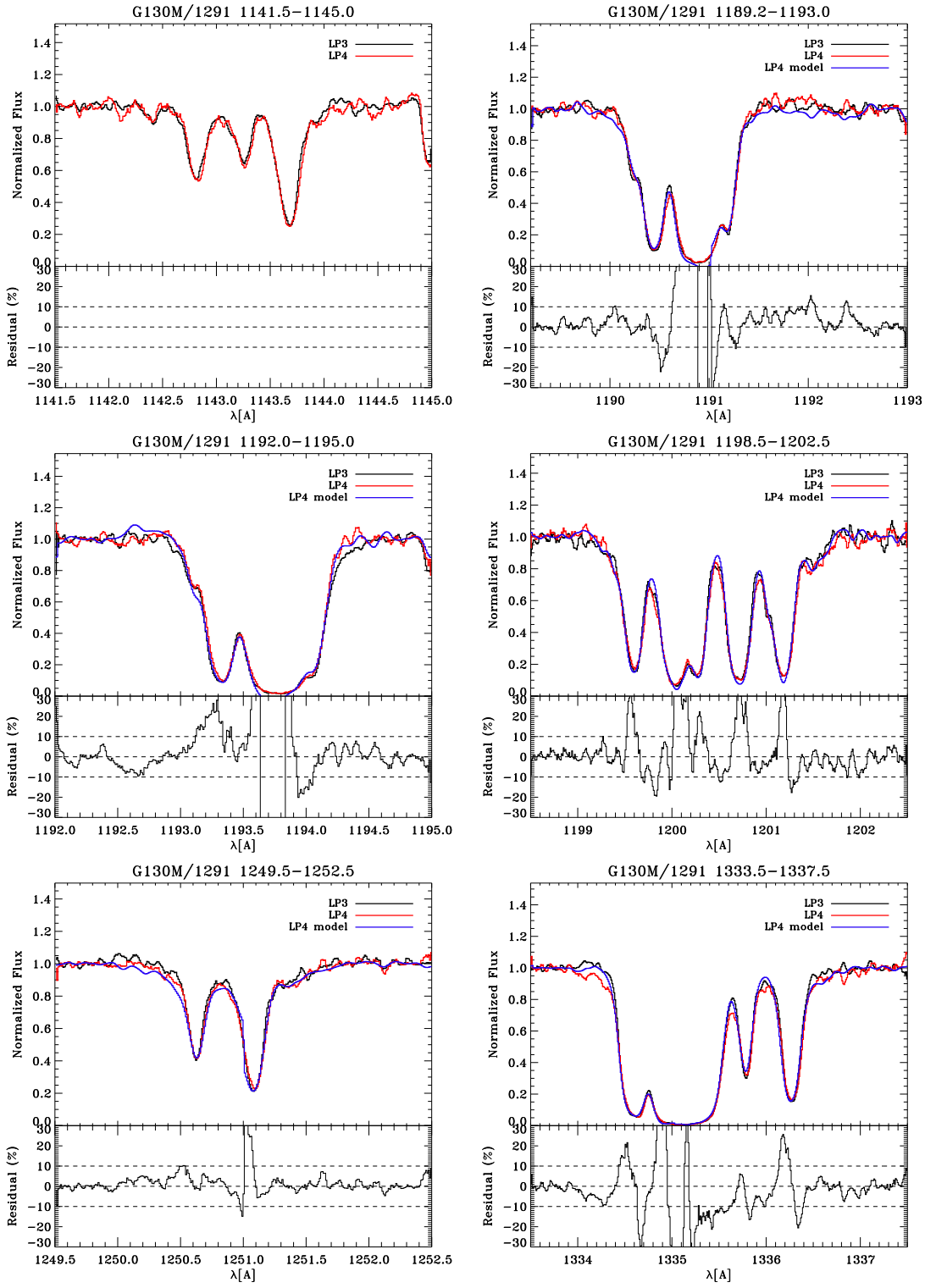

Figure 10. (cont): Comparison of LP3 and LP4 spectra for G130M/1291.

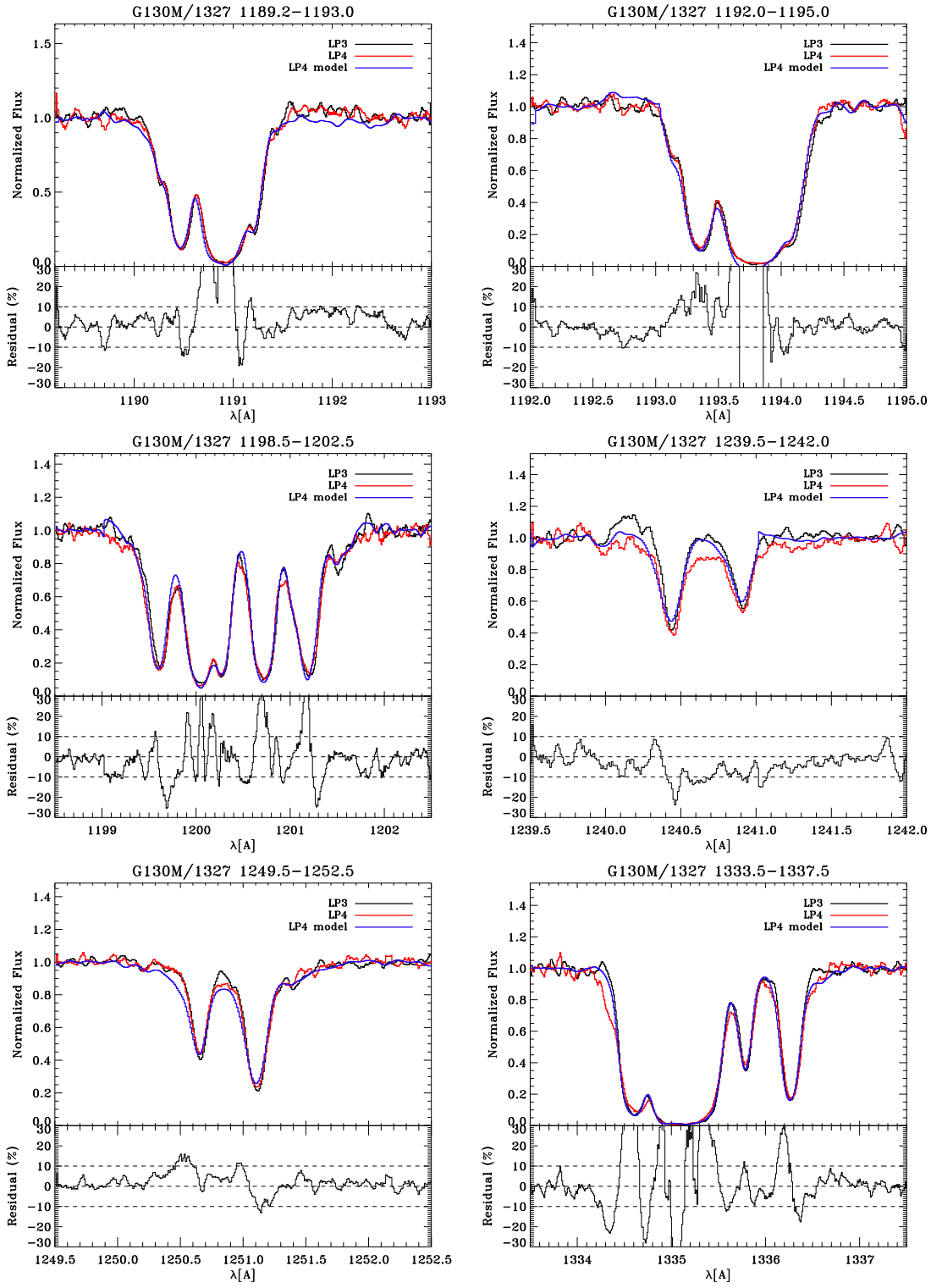

Figure 10. (cont): Comparison of LP3 and LP4 spectra for G130M/1327.

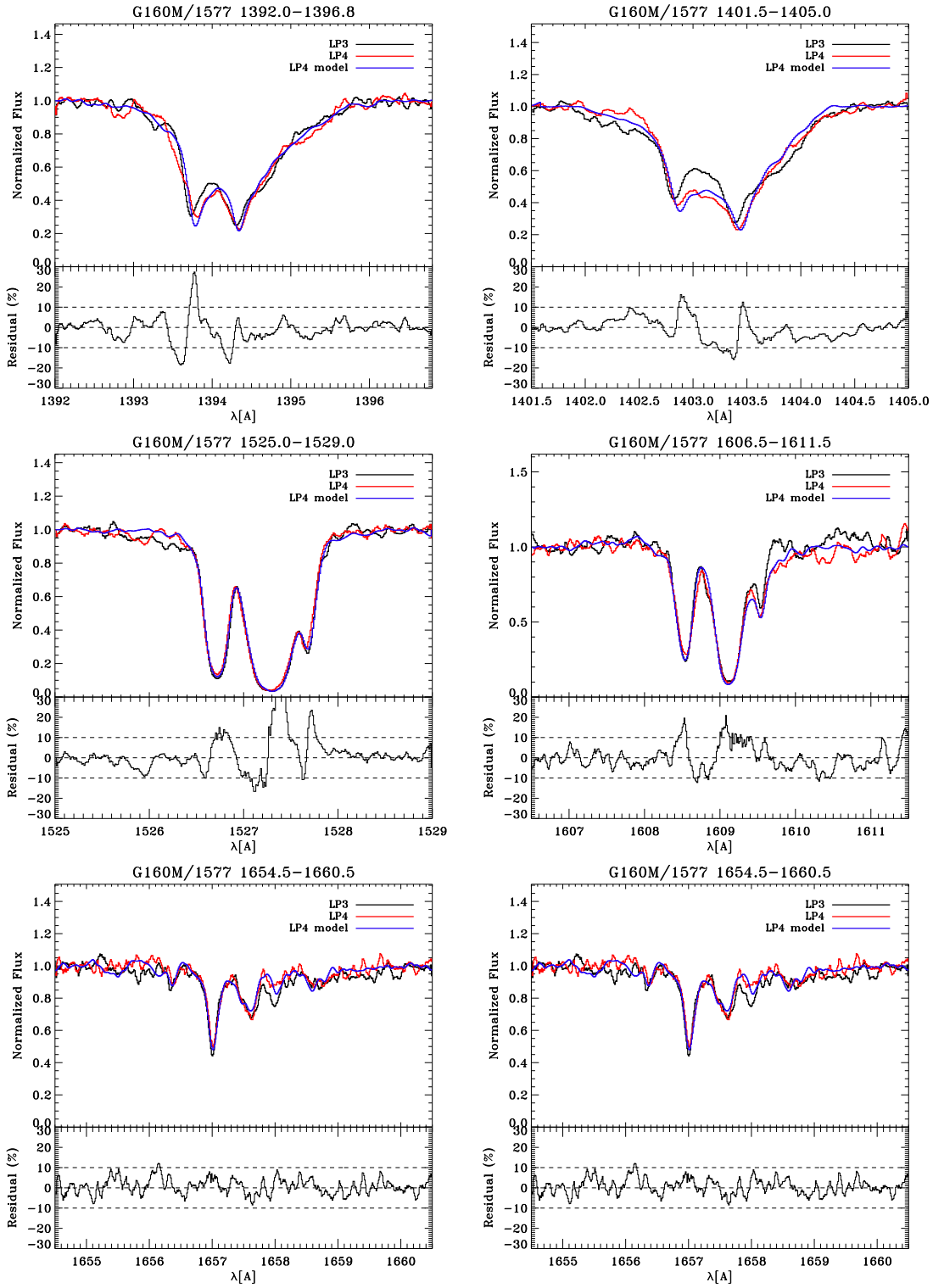

Figure 10. (cont): Comparison of LP3 and LP4 spectra for G160M/1577.

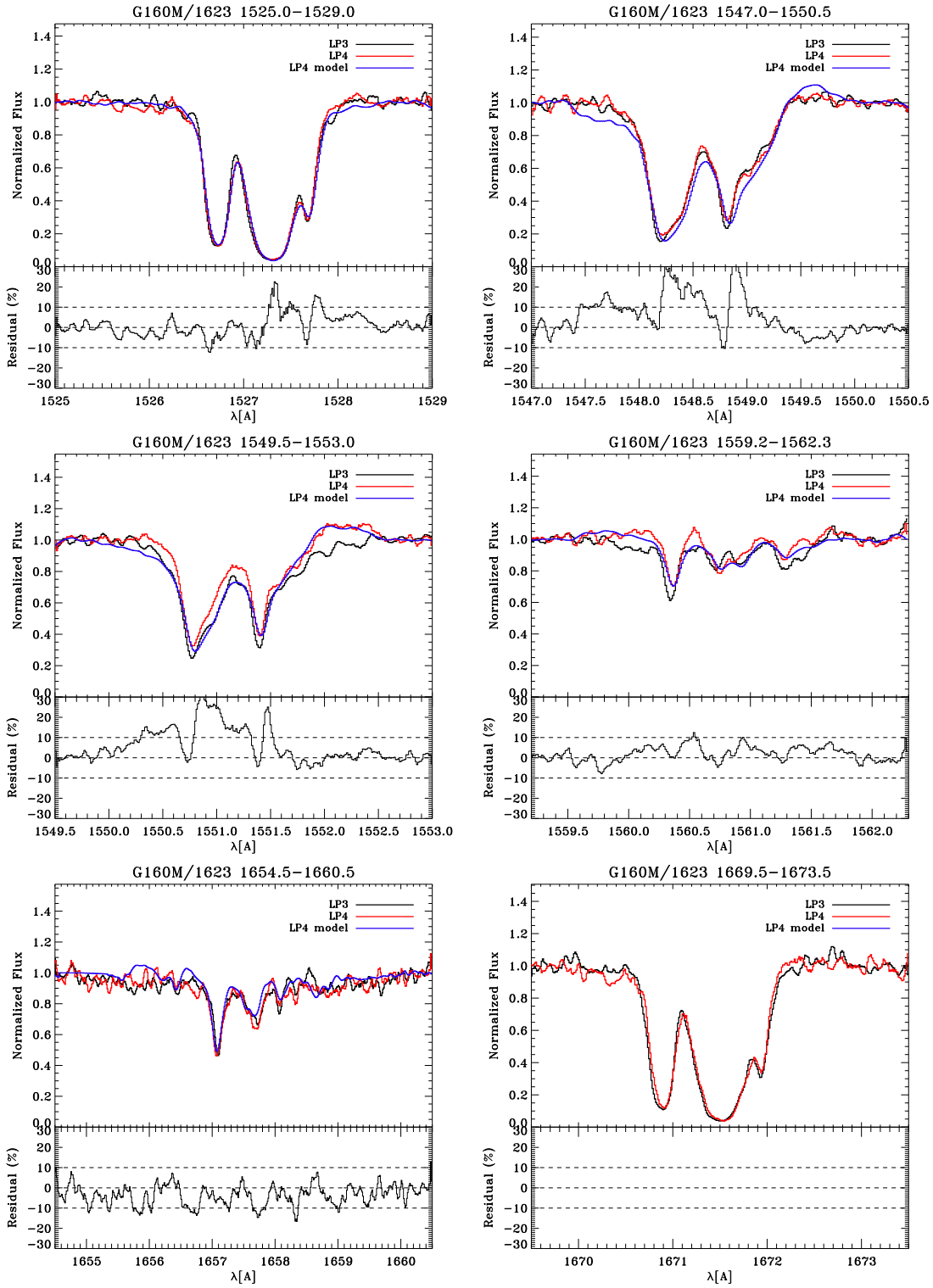

Figure 10. (cont): Comparison of LP3 and LP4 spectra for G160M/1623.